dergo dissociation and reformation.

The $G\alpha_{13}$-Rho pathway participates in phenomena such as cell migration, angiogenesis, and apoptosis (*2*, *3*). The identification of p115 RhoGEF as a critical link in this pathway will facilitate mechanistic understanding of these functions. Furthermore, RGS domains in other proteins may also impart sensitivity to regulation by G protein α subunits.

REFERENCES AND NOTES

1. N. Dhanasekaran and J. M. Dermott, *Cell Signal.* **8**, 235 (1996); A. Hall, *Science* **279**, 509 (1998).
2. A. M. Buhl, N. L. Johnson, N. Dhanasekaran, G. L. Johnson, *J. Biol. Chem.* **270**, 24631 (1995); R. Hooley, C.-Y. Yu, M. Symons, D. L. Barber, *ibid.*, **271**, 6152 (1996); C. Fromm, O. A. Coso, S. Montaner, N. Xu, J. S. Gutkind, *Proc. Natl. Acad. Sci. U.S.A.* **94**, 10098 (1997); H. Althoefer, P. Eversole-Cire, M. I. Simon, *J. Biol. Chem.* **272**, 24380 (1997); S. G. Plonk, S.-K. Park, J. H. Exton, *ibid.*, **273**, 4823 (1998).
3. S. Offermanns, V. Mancino, J.-P. Revel, M. I. Simon, *Science* **275**, 533 (1997).
4. M. S. Boguski and F. McCormick, *Nature* **366**, 643 (1993).
5. R.-G. Qiu, J. Chen, F. McCormick, M. Symons, *Proc. Natl. Acad. Sci. U.S.A.* **92**, 11781 (1995); S. Powers, K. O'Neill, M. Wigler, *Mol. Cell. Biol.* **9**, 390 (1989); S. A. Haney and J. R. Broach, *J. Biol. Chem.* **269**, 16541 (1994).
6. R. A. Cerione and Y. Zheng, *Curr. Opin. Cell Biol.* **8**, 216 (1996); I. P. Whitehead, S. Campbell, K. L. Rossman, C. J. Der, *Biochim. Biophys. Acta* **1332**, F1 (1997).
7. M. J. Hart *et al.*, *J. Biol. Chem.* **271**, 25452 (1996).
8. T. Kozasa *et al.*, *Science* **280**, 2109 (1998).
9. H. G. Dohlman and J. Thorner, *J. Biol. Chem.* **272**, 3871 (1997); M. R. Koelle, *Curr. Opin. Cell. Biol.* **9**, 143 (1997); D. M. Berman and A. G. Gilman, *J. Biol. Chem.* **273**, 1269 (1998).
10. EXV-Myc tagged (for COS cell transfections) and pAc-Glu–tagged (for baculovirus expression) proteins with deletions of the RGS or DH domains have been described previously (*7*). Full-length versions were constructed in the same vectors. Transfection, immunoprecipitation, and purification were performed as described previously (*7*). Cells were lysed in 20 mM tris (pH 7.5), 1 mM dithiothreitol (DTT), 100 mM NaCl, 1 mM EGTA, 5 mM $MgCl_2$, and 0.7% Triton X-100. Where indicated, AMF (50 μM $AlCl_3$, 10 mM $MgCl_2$, and 5 mM NaF) was included.
11. W. D. Singer, R. T. Miller, P. C. Sternweis, *J. Biol. Chem.* **269**, 19796 (1994).
12. D. M. Berman, T. Kozasa, A. G. Gilman, *ibid.*, **271**, 27209 (1996).
13. M. J. Hart, W. Roscoe, G. Bollag, unpublished data.
14. Gα subunits were prepared as described (*8*). RhoA was expressed as a fusion protein (GST-RhoA) in Sf9 cells, followed by affinity purification and removal of the GST tag as described previously [W. D. Singer, H. A. Brown, X. Jiang, P. C. Sternweis, *J. Biol. Chem.* **271**, 4504 (1996)].
15. Dissociation assay. RhoA (2.5 μM) was loaded with [^{3}H]GDP by incubation at 30°C for 1 hour with 25 μM GDP (10,000 cpm/pmol) in 50 mM Na-Hepes (pH 7.5), 50 mM NaCl, 4 mM EDTA, 1 mM DTT, and 0.1% Triton X-100. After addition of $MgCl_2$ to 9 mM and octylglucoside to 1%, Rho was incubated for 5 min at 30°C and separated from free GDP by rapid filtration through Sephadex-G50 that had been equilibrated with 50 mM Na-Hepes (pH 7.5), 50 mM NaCl, 1 mM EDTA, 1 mM DTT, 5 mM $MgCl_2$, and 1% octylglucoside. Dissociation of GDP from RhoA was measured at 30°C in 20 μl of 50 mM Na-Hepes (pH 7.5), 50 mM NaCl, 1 mM EDTA, 1 mM DTT, 5 mM $MgCl_2$, 30 μM $AlCl_3$, 5 mM NaF, and 5 μM GTP-γ-S. Unless specified, G protein α subunits were first incubated with AMF (30 μM $AlCl_3$, 5 mM $MgCl_2$, and 5 mM NaF) before mixing with other proteins. Where indicated, α subunits were incubated for 60 min at 30°C with 25 μM GTP-γ-S or GDP-β-S (rather than AMF), 1 mM EDTA, and 0.5 mM $MgSO_4$, and dissociation assays included 5 μM nucleotide (and no AMF). Reactions were started by addition of [^{3}H]GDP-RhoA, and bound GDP was determined by filtration [J. K. Northup, M. D. Smigel, A. G. Gilman, *J. Biol. Chem.* **257**, 11416 (1982)] before and after incubation.
16. K. Barrett, M. Leptin, J. Settleman, *Cell* **91**, 905 (1997); U. Haecker and N. Perrimon, *Genes Dev.* **12**, 274 (1998).
17. G. Berstein *et al.*, *Cell* **70**, 411 (1992); V. Y. Arshavsky and M. D. Bownds, *Nature* **357**, 416 (1992); V. Z. Slepak *et al.*, *J. Biol. Chem.* **270**, 14319 (1995).
18. G. H. Biddlecome, G. Berstein, E. M. Ross, *J. Biol. Chem.* **271**, 7999 (1996).

19. We thank S. Gutowski and J. Laidlaw for technical assistance. Supported by American Heart Association grant 96G105 (T.K.); the Bayer Corporation (Onyx); NIH grant GM34497 and the Raymond and Ellen Willie Distinguished Chair in Molecular Neuropharmacology (A.G.G.); and NIH grant GM 31954, the Robert A. Welch Foundation, and the Alfred and Mabel Gilman Professorship in Molecular Pharmacology (P.C.S.).

20 March 1998; accepted 7 May 1998

Type IV Pili, Transient Bacterial Aggregates, and Virulence of Enteropathogenic *Escherichia coli*

David Bieber, Sandra W. Ramer, Cheng-Yen Wu, William J. Murray, Toru Tobe, Rosemary Fernandez, Gary K. Schoolnik*

Type IV bundle-forming pili of enteropathogenic *Escherichia coli* are required for the localized adherence and autoaggregation phenotypes. Whether these pili are also required for virulence was tested in volunteers by inactivating *bfpA* or *bfpT* (*perA*) encoding, respectively, the pilus subunit and the *bfp* operon transcriptional activator. Both mutants caused significantly less diarrhea. Mutation of the *bfpF* nucleotide-binding domain caused increased piliation, enhanced localized adherence, and abolished the twitching motility–dispersal phase of the autoaggregation phenotype. The *bfpF* mutant colonized the human intestine but was about 200-fold less virulent. Thus, BfpF is required for dispersal from the bacterial aggregate and for full virulence.

The type IV family of bacterial pili, produced by several human and animal pathogens, is thought to participate in the infectious process by promoting bacterial adherence to host cells (*1*). However, evidence for this putative pathogenic role comes largely from in vitro observations; for the only two species tested in humans, *Neisseria gonorrhoeae* and *Vibrio cholerae* 01, the type IV pili have been shown to be required for infectivity (*2*). Type IV pili are also associated in some bacterial species with twitching motility, a kind of nonflagellar movement thought to promote spread of the organism on body surfaces (*3*). However, the relevance of twitching motility for the infectious process has not been tested.

Enteropathogenic *Escherichia coli* (EPEC) is a type IV pilus–producing biotype and a common cause of childhood diarrhea in developing countries (*4*). Most EPEC serotypes isolated from patients and all experimentally infectious strains harbor an ~80-kb enteroadherence factor (EAF) plasmid (*5–7*) containing an operon that encodes a type IV pilus—designated the bundle-forming pilus (BFP)—because pilus filaments emanating from the bacterial surface appear to align along their longitudinal axes to form bundles of filaments (Fig. 1A) (*8*, *9*). BFP expression is induced during logarithmic-phase growth and regulated by physicochemical signals characteristic of the small intestine (*10*). BFP biogenesis is directed by an operon of 14 genes (*9*, *11*), including *bfp*A, which encodes the major repeating subunit of the pilus fiber (*12*). A transcriptional factor encoded by the *bfpT* (also called *perA*) operon is required for *bfp* operon expression and is located elsewhere on the EAF plasmid (*13*, *14*).

BFP expression is required for the development of EPEC microcolonies on tissue culture cell monolayers [the localized adherence (LA) phenotype] (*5*, *8*) and the formation of spherical bacterial aggregates in tissue culture media (the autoaggregation phenotype) (*15*). The latter is distinct from the "aggregative adherence" phenotype exhibited by some enteroaggregative *E. coli* in that the EPEC autoaggregation phenotype

D. Bieber, S. W. Ramer, C.-Y. Wu, R. Fernandez, G. K. Schoolnik, Department of Medicine, Division of Infectious Diseases and Geographical Medicine, and Department of Microbiology and Immunology, Stanford Program for Vaccine Research, Stanford University Medical Center, Stanford, CA 94305 USA.
W. J. Murray, Department of Biological Sciences, San Jose State University, San Jose, CA 95912 USA.
T. Tobe, Department of Bacteriology, Institute of Medicine, University of Tokyo, Tokyo, Japan.

*To whom correspondence should be addressed. E-mail: ml.gks@forsythe.stanford.edu

occurs in the absence of eukaryotic cells or other substrata (*16*). The plausible in vivo correlation of the LA phenotype is mucous membrane adherence, whereas the role of the autoaggregation phenotype, if any, is enigmatic.

The chromosomal locus of enterocyte effacement (LEE) is required for actin condensation, resulting in localized elevation and invagination of the epithelial cell plasma membrane (pedestal formation), a histological feature of EPEC infection in children (*17, 18*). Disruption of one LEE region gene, *eaeA*, which encodes the protein intimin, reduces but does not abolish virulence (*7*). Another gene of the LEE region, *tir*, is proposed to serve as the bacteria-encoded receptor for intimin (*19*), although its role in virulence is untested.

Two multistep models of EPEC pathogenesis have been proposed. In one, BFP initiates adherence by serving as a long-range adhesin (*20*); in the other, they recruit other EPEC into a growing microcolony after an individual bacterium first forms a pathogenic union with the intestinal epithelium (*21*). The common pathway for both models is intimin-mediated attachment of EPEC to the enterocyte followed by bacteria-to-cell signaling events, which trigger actin condensation (*20, 21*), cellular dysfunction, and diarrhea.

We measured the effects of mutations within the *bfp* operon on the diarrheal response of orally inoculated volunteers to test two predictions of these models: (i) a BFP-negative mutant will be avirulent, and (ii) an adherence-competent EPEC that causes actin condensation and pedestal formation in tissue culture cells will cause diarrhea in humans. Two mutations of the wild-type EPEC strain B171-8 (serotype O111:NM) were constructed, yielding mutants B171-8ΔAcm, which interrupts *bfpA*, and B171-8T::Gm, which inactivates *bfpT*; neither makes BFP or its structural subunit (*22*). Healthy adult volunteers drank 5×10^8, 2.5×10^9, or 2×10^{10} colony-forming units (CFUs) of the wild-type parent or one of the two BFP-negative mutants, assigned according to a randomized, double-blind experimental design (*23*). The volume of liquid stool passed during the next 48 hours served as the primary end point. Volunteers receiving different-sized inocula of the wild-type strain exhibited a dose-dependent diarrheal response: the average volumes of liquid stool were 376, 1104, and 3437 ml for volunteers receiving 5×10^8, 2.5×10^9, and 2×10^{10} CFUs, respectively (Fig. 2, red bars). In total, 11 of the 13 volunteers challenged with the wild-type strain developed clinical diarrhea. By contrast, only 2 of 16 volunteers ($P = 0.0001$) receiving the B171-8ΔAcm mutant experienced diarrhea, including 0 of 6 who received the highest inoculum (Fig. 2, green bars). Similarly, only 3 of 14 volunteers ($P = 0.001$) receiving the B171-8T::Gm mutant experienced diarrhea; their illness was mild, consisting of a single liquid stool in 3 of the 4 persons receiving the highest challenge dose (Fig. 2, purple bars). Thus, the BFP is an EPEC virulence determinant.

To learn more about BFP biogenesis and function, the putative nucleotide-binding domains of *bfpD* and *bfpF* were mutated. These *bfp* operon genes have been proposed to provide energy for pilus biosynthesis (*9, 24*). *pilT* homologs in *N. gonorrhoeae* and *Pseudomonas aeruginosa* also code for putative nucleotide-binding proteins that are required for the twitching motility phenotype of these species (*25*). We carried out site-directed mutagenesis of the Walker box

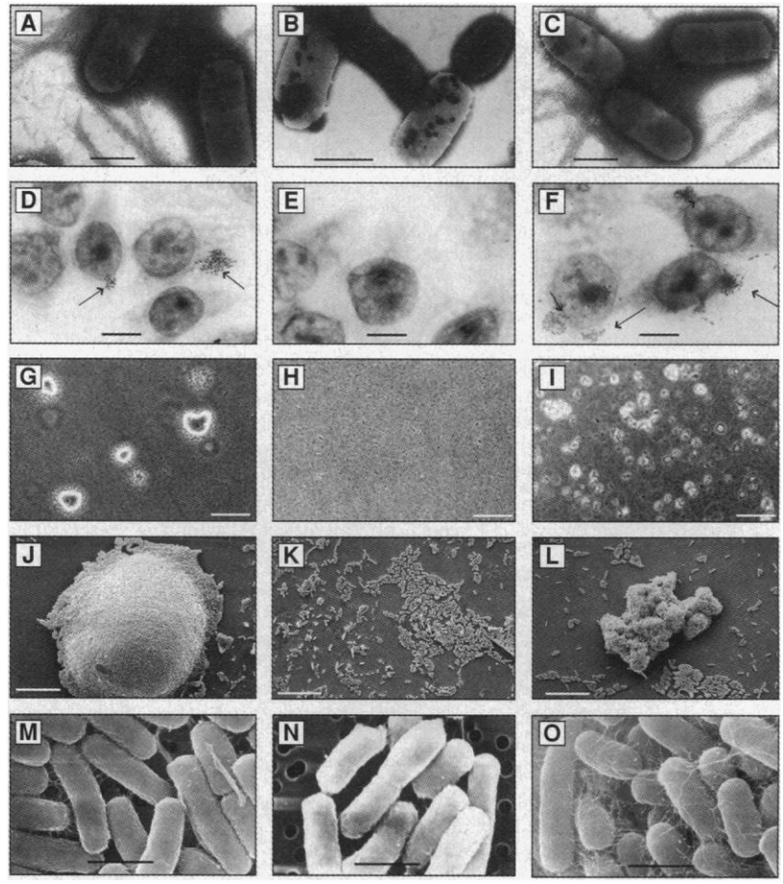

Fig. 1. In vitro phenotypes exhibited by wild-type EPEC strain B171-8 and mutants of this strain: wild-type B171-8 (A, D, G, J, and M); the three BFP-negative mutants B171-8ΔAcm, B171-8T::Gm, and B171-8ΔD (B,E,H,K,N); and the two BfpF-mutants, B171-8ΔF and B171-8F^{ma} (C, F, I, L, and O). (**A** to **C**) Negatively stained immunogold transmission electron micrographs (TEMs) of these EPEC variants, labeled with rabbit antibody to BFP followed by goat immunoglobulin G to rabbit conjugated with 10-nm gold particles. BFP appear as gold-labeled, laterally aligned filaments (A and C). The BFP-negative mutants lack gold-labeled filaments (B). Bars = 0.6 μm. (**D** to **F**) The LA phenotype, characterized by microcolonies attached to the surface of cultured HEp-2 cells, is expressed by B171-8 (D) and the F mutant, B171-8F^{ma} (arrows) (F); the BFP-negative mutants are LA-phenotype negative (E). Bars =10 μm. (**G** to **I**) The autoaggregation phenotype 3 hours after diluting a standard overnight culture of EPEC 1:100 into DMEM (*10*). Phase-contrast micrographs (×10 objective) of hanging drop samples: BFP-negative mutants do not form discrete bacterial assemblages (H); B171-8 forms autoaggregates (G); the F mutants of B171-8 associate as irregular, refractile clumps, designated autoagglutinates (I). Bars = 100 μm. (**J** to **L**) SEM images of the autoaggregation assay. Three-hour DMEM cultures [using bacteria prepared as in (G) to (I)] were fixed in gluteraldehyde, collected onto polycarbonate filters, washed, postfixative stained with osmium tetroxide, dehydrated in a graded alcohol series, critical-point dried, and sputter coated with iridium. Wild-type B171-8 autoaggregates appear as smooth domes (J), whereas the F mutants, B171-8F^{ma}, form irregular autoagglutinates (L). BFP-negative mutants, B171-8ΔAcm, are arrayed as individual bacteria, small groups of bacteria, or flat bacterial mats (K). Bars = 20 μm. (**M** to **O**) SEM images of the same samples depicted in (J to L) demonstrating the paucity of fibers in the BFP-negative samples (N) and the hyperpiliated B171-8F^{ma} mutant (O) relative to the BFP fibers produced by the wild-type strain (M). Bars = 1.2 μm.

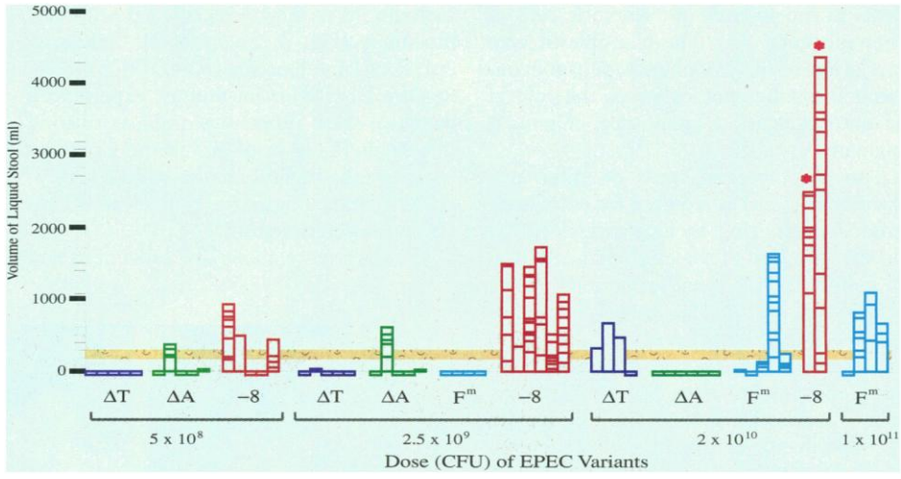

Fig. 2. Comparative virulence of EPEC strain B171-8 and mutants of this strain at different bacterial doses as measured by the diarrheal response of orally challenged volunteers. All stools passed by volunteers were collected, weighed, and scored as formed/semiformed or liquid (taking the shape of the container). Diarrhea was defined as one liquid stool of 300 ml or more, or two or more liquid stools totaling 200 ml or more (indicated by the shaded horizontal band between 200 and 300 ml) during a 48-hour period after ingestion of the challenge bacteria. Each vertical bar represents an individual volunteer; bars below the abscissa represent individuals who produced no liquid stools during the first 48 hours. Heights of the individual bars show the cumulative volume of liquid stool (milliliters) during the study period. Horizontal hash marks within each bar depict the volume of each successive liquid stool. The four bacterial challenge doses, designated in CFUs, are shown beneath the brackets enclosing the bacterial variants administered at that dose. Symbols under each cluster of individual bars within a dosage group denote the variant administered: ΔT (purple bars) denotes B171-8T::Gm, the *bfpT* disruption mutant; ΔA (green bars) denotes B171-8ΔAcm, the *bfpA* deletion mutant; F^m (blue bars) denotes B171-$8F^{ma}$, the site-directed mutant of *bfpF*; and −8 (red bars) denotes B171-8, the wild-type parental EPEC strain. Mean stool volumes of each group were compared by Student's two-tailed *t* test: all ΔT versus all −8, $P = 0.007$; all ΔA versus all −8, $P = 0.006$; all F^{ma} versus all −8, $P = 0.03$. Only two volunteers (red * above bars) developed symptoms severe enough to warrant halting the experiment, both at hour 14.

A consensus sequence GXXGXGKT/S (*26*) located between residues 260 and 267 of BfpD and between residues 131 and 141 of BfpF and thought to form a loop structure in which the lysine residue directly contacts the phosphoryl group of the bound nucleotide (*27*). Within this motif, we changed both G^{265} to A^{265} and K^{266} to R^{266} of BfpD to yield the mutant B171-$8D^{G265A,K266R}$ (henceforth abbreviated B171-$8D^{ma}$) and G^{139} to A^{139} and K^{140} to R^{140} to yield the mutant B171-$8F^{G139A,K140R}$ (henceforth abbreviated B171-$8F^{ma}$) (*28*).

The *bfpD* mutant, B171-$8D^{ma}$, did not express BFP, did not autoaggregate, and was LA phenotype negative. Thus, BfpD is required for BFP biogenesis. By contrast, the *bfpF* mutant, B171-$8F^{ma}$, expressed BFP and attached to cultured HEp-2 cell monolayers in a pattern that resembled, but was not identical to, the LA phenotype of the wild-type parent strain. Visualization of multiple fields revealed that B171-$8F^{ma}$ was more adherent than the parent strain, similar to a B171-8ΔF mutant that we constructed (*16*, *28*) and to a *bfpF* deletion mutant of EPEC strain E2348/69, which was reported to be eightfold more adherent than the parent (*24*). Phase-contrast microscopy of B171-$8F^{ma}$ and B171-8ΔF showed that they formed bacterial aggregates that were morphologically distinct from the aggregates produced by the parent strain (Fig. 1, G to I). In particular, whereas the autoaggregates formed by wild-type bacteria disperse over time, BfpF mutant bacteria remained clumped—a *bfpF*-specific phenotype that we term autoagglutination. Western blot analysis of B171-$8F^{ma}$ and B171-8 showed similar levels of BfpF and the corresponding mutant protein, indicating that the resulting phenotype changes are likely due to loss of normal Walker box A–mediated functions.

The effect of the B171-$8F^{ma}$ mutation appears to dissociate two BFP-associated phenotypes: LA, which is preserved or enhanced, and AA, which is altered in the mutant by its inability to dissociate from the aggregate. To better understand the significance of these seemingly subtle differences, we asked three questions about this mutant: what is the difference between autoaggregation and autoagglutination, does B171-$8F^{ma}$ cause actin condensation and thus exhibit LEE-region associ-

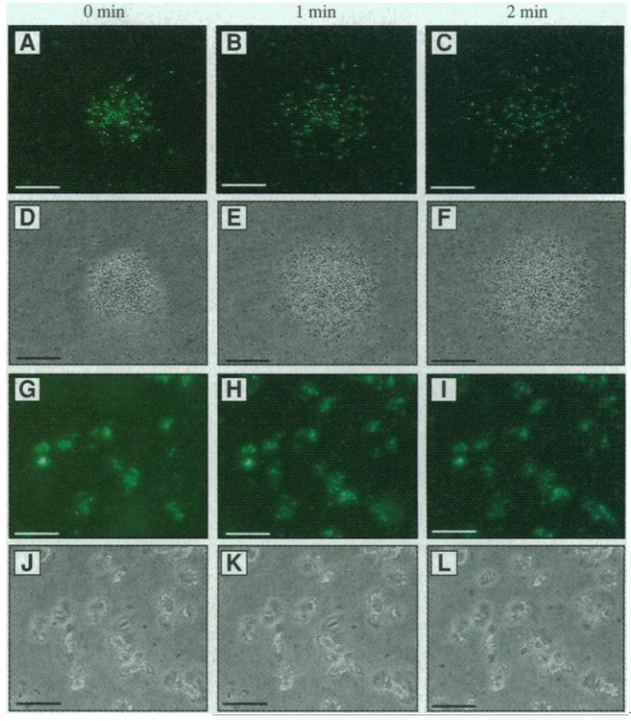

Fig. 3. Time-lapse fluorescence and phase-contrast photomicrographs of the dispersal phase of the EPEC autoaggregation phenotype. Wild-type (**A** to **F**) or BfpF mutant (**G** to **L**) EPEC bacteria were grown with shaking in DMEM at 37°C for 3 hours to produce autoaggregates (wild-type bacteria) or autoagglutinates (BfpF mutant). Each culture was inoculated with a 50:1 ratio of unlabeled and GFP-expressing bacteria of the same type (wild type or mutant). Hanging-drop samples of the cultures were examined by fluorescence microscopy (A to C and G to I) to visualize individual GFP-labeled bacteria or by phase-contrast microscopy (D to F and J to L) to visualize the bacterial aggregates and agglutinates. Images of the same field and in the same focal plane were collected every minute as the samples cooled from 37°C to room temperature. Wild-type bacteria rapidly disperse from the dissociating aggregate, whereas BfpF mutant bacteria form stable agglutinates.

ated functions, and is it virulent?

Autoaggregates of the wild-type parent and autoagglutinates of B171-8F^{ma} were studied by immunogold transmission electron microscopy, phase-contrast microscopy, and scanning electron microscopy (Fig. 1). Bundles of gold-labeled pilus filaments, evident within autoaggregates as well as autoagglutinates, appeared to form interbacterial linkages (Fig. 1, A to C). No consistent difference between wild-type and mutant was detected in the configuration of pilus filaments or in interbacterial distances. However, high-resolution scanning electron micrographs (SEMs) showed that the BfpF mutants produced many more interbacterial filaments than the wild-type parent strain (Fig. 1, M to O). Low-power views of the same assemblages showed dramatic differences in the architecture of the two aggregates: the wild-type strain produced smoothly contoured domes, whereas the agglutinates of the BfpF mutant had a highly irregular surface (Fig. 1, J to L).

Differences in the dynamic formation and dispersal of bacterial aggregates and agglutinates were monitored by labeling either the wild-type strain or B171-8F^{ma} with green fluorescent protein (GFP) produced from a constitutively expressed copy of that gene (*29*), mixing unlabeled and labeled bacteria of the same type, and observing populations by time-lapse photography (Fig. 3). These images showed that cultivation of the wild-type strain under optimal *bfp* operon-inducing conditions (*10*) resulted in formation of bacterial aggregates during the last 4 hours of exponential-phase growth in Dulbecco's modified Eagle's medium (DMEM); dispersal of the bacteria composing these aggregates ensued, resulting in a suspension of individual bacteria. Within the aggregate, bacteria appeared to move randomly; however, neither this motion nor the active dispersal of bacteria from the aggregate could be ascribed to flagella, because B171-8 is a nonflagellate strain. By contrast, although the time course of autoagglutination by B171-8F^{ma} and autoaggregation by the wild-type strain were similar, the autoagglutinates of B171-8F^{ma} were static assemblages that did not disperse (Fig. 3).

To determine whether differences between the autoaggregation and autoagglutination phenotypes might be correlated with differences in virulence, we challenged volunteers with different doses of B171-8F^{ma} and compared the results with the diarrheal response induced by the wild-type strain. The results, (Fig. 2, light blue bars) showed that the *bfpF*^{ma} mutant was significantly attenuated in its ability to cause diarrhea (only 4 of 13 volunteers developed diarrhea; $P = 0.003$), effectively shifting the dose-response curve to the right, so that ~200-fold more CFUs of B171-8F^{ma} were required to produce the same diarrheal response as the wild-type.

The attenuating effect of the *bfpF*^{ma} mutation could have been due to the inability of the mutant to either colonize the host or, alternatively, to cause the actin condensation postulated to be required for diarrhea. Both the wild-type and *bfpF*^{ma} mutant infected the intestine as evidenced by their presence in stool specimens from a random subset of the volunteers. Thus, this mutation dissociated infectivity (which was retained) from virulence (which was reduced), although our results do not exclude the possibility that mutant and wild-type colonized different regions of the intestine. Further, B171-8F^{ma} retained its capacity to cause actin condensation and pedestal formation, the ultrastructural hallmark of EPEC pathogenesis (Fig. 4). Thus, B171-8F^{ma} had intact LEE region–mediated functions, and these functions elicited the expected responses in HEp-2 cells.

Functional BFP was thus shown to be required for production of diarrhea. Of the five EPEC phenotypes monitored here—LA, actin condensation, intestinal colonization, virulence, and autoaggregation—only the last two were altered by the *bfpF*^{ma} mutation. Possibly each phase of the autoaggregation phenomenon—formation and dispersal—is required for virulence. The first phase might favor bacterial adherence to the epithelial surface as stable, attached microcolonies. During aggregation, physically mediated or chemically mediated signaling (*30*) might occur, stimulating the expression of additional virulence genes. Release of these organisms during the dispersal phase—which may be the EPEC equivalent of twitching motility—could lead to the colonization of additional epithelial sites by these newly programmed bacteria. However, to dissociate from the aggregate, bacteria would need to shed or disentangle their pilus filaments from each other, a process that may require BfpF-mediated, energy-dependent pilus retraction or a conformational change of pilus quaternary structure.

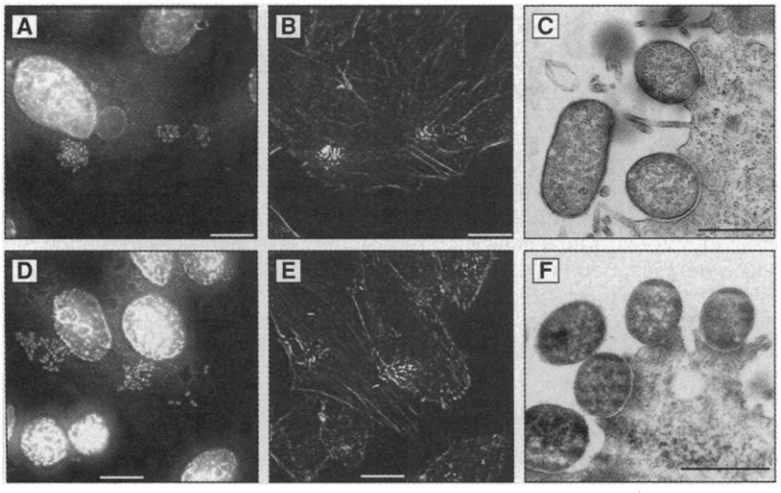

Fig. 4. Pedestal formation and actin condensation induced by wild-type EPEC (**A** to **C**) and the BfpF mutant (**D** to **F**). HEp-2 cells were cocultured with EPEC bacteria for 2 hours in DMEM containing 0.5% mannose (*10*); unattached bacteria were removed by extensive washing with phosphate-buffered saline; and the cells were fixed in formalin, permeabilized with 0.1% Triton X-100, and then labeled with 4′,6′-diamidino-2-phenylindole (A and D) to stain nuclear material and localize the bacteria (clusters of small bright spots) and with BODIPY-phallacidin (B and E) to stain condensed actin (bright flecks colocalizing with EPEC clusters). Lightly stained actin cables can also be seen coursing through the HEp-2 cells. Similarly infected HEp-2 cells were fixed in 2% gluteraldehyde, embedded in LR White, sectioned, and examined by TEM for pedestal formation, characterized by elevation and invagination of the HEp-2 cell plasma membrane. No differences in actin condensation or pedestal formation are evident between wild-type parent (C) and BfpF mutant (F). Bars = 10 μm in (A), (B), (D), and (E) and 1 μm in (C) and (F).

REFERENCES AND NOTES

1. P. A. Manning and T. F. Meyer, Eds., *Gene* **192**, 1 (1997).
2. D. A. Herrington *et al.*, *J. Exp. Med.* **168**, 1487 (1988); J. Swanson and J. M. Koomey, in *Mobile DNA*, D. E. Berg and M. M. Howe, Eds. (American Society for Microbiology, Washington, DC, 1989), pp. 743–761.
3. J. Henrichsen, *Annu. Rev. Microbiol.* **37**, 81 (1983).
4. M. S. Donnenberg, in *Infections of the Gastrointestinal Tract*, M. J. Blaser, P. D. Smith, J. I. Ravdin, H. B. Greenberg, R. L. Guerrant, Eds. (Raven Press, New York, 1995), pp. 709–726.
5. M. M. Baldini, J. B. Kaper, M. Levine, D. Candy, H. Moon, *J. Pediatr. Gastroenterol. Nutr.* **2**, 534 (1983); M. M. Baldini, J. P. Nataro, J. B. Kaper, *Infect. Immun.* **52**, 334 (1986); A. Cravioto, R. Gross, S. Scotland, B. Rowe, *Curr. Microbiol.* **3**, 95 (1979); I. C. Scaletsky, M. Silva, L. Trabulsi, *Infect. Immun.* **45**, 534 (1984); J. P.

Nataro, K. Maher, P. Mackie, J. Kaper, *ibid.* **55**, 2370 (1987); J. P. Nataro, I. Scaletsky, J. Kaper, M. Levine, L. Trabulsi, *ibid.* **48**, 378 (1985).
6. M. M. Levine *et al.*, *J. Infect. Dis.* **152**, 550 (1985).
7. M. S. Donnenberg *et al.*, *J. Clin. Invest.* **92**, 1412 (1993).
8. J. A. Giron, A. S. Y. Ho, G. K. Schoolnik, *Science* **254**, 710 (1991).
9. I. Sohel *et al.*, *J. Bacteriol.* **178**, 2613 (1996); K. D. Stone, H.-Z. Zhang, L. K. Carlson, M. S. Donnenberg, *Mol. Microbiol.* **20**, 325 (1996).
10. J. L. Puente, D. Bieber, S. W. Ramer, W. Murray, G. K. Schoolnik, *Mol. Microbiol.* **20**, 87 (1996).
11. S. W. Ramer, D. Bieber, G. K. Schoolnik, *J. Bacteriol.* **178**, 6555 (1996).
12. I. Sohel, J. L. Puente, W. J. Murray, J. Vuopio-Varkila, G. K. Schoolnik, *Mol. Microbiol.* **7**, 563 (1993); M. S. Donnenberg, J. A. Giron, J. P. Nataro, J. B. Kaper, *ibid.* **6**, 3427 (1992).
13. T. Tobe, G. K. Schoolnik, I. Sohel, V. H. Bustamante, J. L. Puente, *ibid.* **21**, 963 (1996).
14. O. G. Gomez-Duarte and J. B. Kaper, *Infect. Immun.* **63**, 1767 (1995).
15. J. Vuopio-Varkila and G. K. Schoolnik, *J. Exp. Med.* **174**, 1167 (1991).
16. D. Bieber, S. W. Ramer, C.-Y. Wu, unpublished results.
17. R. Rothbaum, A. McAdams, R. Giannella, J. Partin, *Gastroenterology* **83**, 441 (1982); S. M. Hill, A. D. Phillips, S. J. Walker, *Gut* **32**, 154 (1991); C. J. Taylor, A. Hart, R. M. Batt, C. McDougall, L. McLean, *J. Pediatr. Gastroenterol. Nutr.* **5**, 70 (1986); A. E. Jerse, J. Yu, B. D. Tall, J. B. Kaper, *Proc. Natl. Acad. Sci. U.S.A.* **87**, 7839 (1990); A. E. Jerse, K. G. Gicquelais, J. B. Kaper, *Infect. Immun.* **59**, 3869 (1991); T. K. McDaniel, K. G. Jarvis, M. S. Donnenberg, J. B. Kaper, *Proc. Natl. Acad. Sci. U.S.A.* **92**, 1664 (1995); T. K. McDaniel and J. B. Kaper, *Mol. Microbiol.* **23**, 399 (1997).
18. S. Knutton, T. Baldwin, P. H. Williams, A. S. McNeish, *Infect. Immun.* **57**, 1290 (1989).
19. B. Kenny *et al.*, *Cell* **91**, 511 (1997).
20. M. S. Donnenberg, J. B. Kaper, B. B. Finlay, *Trends Microbiol.* **5**, 109 (1997).
21. S. Hicks, G. Frankel, J. B. Kaper, G. Dougan, A. D. Phillips, *Infect. Immun.* **57**, 1570 (1998).
22. Mutations were introduced into the EAF plasmid by homologous recombination after first introducing the gene-specific changes into the respective fragments subcloned into pBlueScript (Stratagene). We used a limited polymerase chain reaction (PCR)–based mutational strategy to reduce the chance of introducing secondary mutations; minimal regions of the PCR-amplified products containing the desired changes were ligated into existing subclones. The limited PCR regions could easily be sequenced and shown to be free of extraneous mutations. To generate the desired alteration on the EAF plasmid in B171-8, we performed suicide vector–directed homologous double recombination as described in (*7, 11*). We generated B171-8ΔAcm by replacing the pilinencoding *bfpA* gene with a chloramphenicol acetyltransferase gene; transcription of the remaining *bfp* operon genes was unaffected (*11, 16*). B171-8T::Gm has sustained an insertional disruption of *bfpT* (*13*). Wild-type phenotypes were restored by providing the mutants with a normal copy of the respective gene in trans on a low-copy-number plasmid.
23. Healthy adult volunteers (18 to 48 years old) gave written, informed consent for participation in this study. All volunteers provided a medical history and underwent physical examination and laboratory testing. The study was performed in the General Clinical Research Center (GCRC) at Stanford Hospital (Stanford University, Palo Alto, CA). The challenge organisms were resuscitated from frozen stocks of organisms that were confirmed to be O111 antiserum reactive, EAF plasmid positive, and *eaeA* hybridization positive. Each mutant carried its characteristic mutation as assessed by DNA sequence, mRNA, and protein immunoblot analysis. The cultures were grown overnight in Luria broth, washed three times in phosphate-buffered saline (0.85%), visually inspected for the absence of bacterial clumps, and adjusted to the appropriate OD_{600} for each inoculation. Volunteers took nothing by mouth for 2 hours before challenge. They ingested 150 ml of a 1.3% sodium bicarbonate solution 1 minute before ingesting 30 ml of the dose of challenge bacteria in phosphate-buffered saline plus 1.3% sodium bicarbonate. All stool samples were collected for 48 hours. The nursing staff were unaware of the nature of the challenge bacteria and scored the stool specimens as formed/semiformed or liquid. The end point of this study was development of diarrhea as indicated by the volume and number of liquid stools produced in the first 48 hours. Forty-eight hours after ingesting the bacteria the volunteers were treated with ciprofloxacin and were released from the GCRC after their stools were determined to be negative for *E. coli*.
24. R. P. Anantha, K. D. Stone, M. S. Donnenberg, *Infect. Immun.* **66**, 122 (1998).
25. C. B. Whitchurch, M. Hobbs, S. P. Livingston, V. Krishnapillai, J. S. Mattick, *Gene* **101**, 33 (1991); P. Lauer, N. H. Albertson, M. Koomey, *Mol. Microbiol.* **8**, 357 (1993).
26. Amino acid residues are abbreviated as follows: A, Ala; C, Cys; D, Asp; E, Glu; F, Phe; G, Gly; H, His; I, Ile; K, Lys; L, Leu; M, Met; N, Asn; P, Pro; Q, Gln; R, Arg; S, Ser; T, Thr; V, Val; W, Trp; X, Xaa; Y, Tyr.
27. D. C. Fry, S. A. Kuby, A. S. Mildvan, *Proc. Natl. Acad. Sci. U.S.A.* **83**, 907 (1986); S. C. Hyde *et al.*, *Nature* **346**, 362 (1990).
28. In-frame deletion mutations of *bfpD* (B171-8ΔD) and *bfpF* (B171-8ΔF) were constructed from convenient restriction sites within those genes. Site-directed mutations in the nucleotide triphosphate binding regions of BfpD (B171-8D^{ma}) and BfpF (B171-8F^{ma}) were generated by a modification of the Stratagene QuikChange mutagenesis strategy. A pair of primers carrying the intended nucleotide changes but otherwise complementary to the sequences encoding the Walker box A region of either protein were used for amplification. To minimize unintentional changes in the nucleotide sequence, we used the limited PCR-based strategy (*22*) to replace the homologous wild-type fragment that had been cloned into a modified version of suicide plasmid pGP704 (*31*). The appropriate loci of the EAF plasmid were replaced by the intended mutations by using the suicide vector–driven homologous recombination strategy employed above. Complementation of the D and F mutations was accomplished by providing a copy of the wild-type gene on a low-copy-number plasmid, which restored the normal LA and autoaggregation phenotypes.
29. R. H. Valdivia and S. Falkow, *Mol. Microbiol.* **22**, 367 (1996).
30. D. G. Davies *et al.*, *Science* **280**, 295 (1998); W. C. Fuqua, S. C. Winans, E. P. Greenberg, *J. Bacteriol.* **176**, 269 (1994); S. Swift, J. P. Throup, P. Williams, G. P. Salmond, G. S. Stewart, *Trends Biochem. Sci.* **21**, 214 (1996).
31. V. L. Miller and J. J. Mekalanos, J. Bacteriol. **170**, 2575 (1988).
32. Scanning electron microscopy was performed at the Microscope and Graphic Imaging Center, California State University, Hayward (N. R. Smith, Director) and at the SETI Institute, NASA Ames Research Center. The studies of volunteers were performed in the General Clinical Research Center (GCRC) at Stanford University Medical Center. Supported by Health and Human Services grants 1R03-DK52038 and 1R01-AI39521 from the National Institutes of Health and by Health and Human Services grant M01-RR00070 from the General Clinical Research Program, National Institutes of Health. We thank D. Kaiser, B. Stocker, and B. W. Brown for helpful suggestions and critical reading of the manuscript; R. Valdivia and S. Falkow for providing the GFP plasmid; S. R. Kushner for providing pWKS plasmids; J. Giron for providing the BFP antiserum; J. Engel for the suggestion to use GFP to mark the individual bacteria; the nursing staff of the GCRC and the volunteers for their participation in the study; and N. Smith and K. Kato for their advice and generous use of the SEMs.

27 February 1998; accepted 11 May 1998

Drosophila Synapse Formation: Regulation by Transmembrane Protein with Leu-Rich Repeats, CAPRICIOUS

Emiko Shishido, Masatoshi Takeichi, Akinao Nose*†

Upon reaching the target region, neuronal growth cones transiently search through potential targets and form synaptic connections with only a subset of these. The *capricious* (*caps*) gene may regulate these processes in *Drosophila*. *caps* encodes a transmembrane protein with leucine-rich repeats (LRRs). During the formation of neuromuscular synapses, *caps* is expressed in a small number of synaptic partners, including muscle 12 and the motorneurons that innervate it. Loss-of-function and ectopic expression of *caps* alter the target specificity of muscle 12 motorneurons, indicating a role for *caps* in selective synapse formation.

The final step in formation of neural connectivity involves the recognition of target cells. Although earlier events of growth cone guidance greatly restrict the target region, neurons still have to choose a specific synaptic partner from among several potential targets (*1*). We studied synapse formation in the neuromuscular system of *Drosophila melanogaster*. In each abdominal hemisegment of *Drosophila* larvae, ~40 motorneurons innervate 30 muscle fibers in a specific manner (*2*). Once a motor axon enters its target region during late embryogenesis, its growth cone searches over the surface of many muscles but withdraws from most of these contacts, forming stable synapses only with its own target or

E. Shishido and A. Nose, National Institute for Basic Biology, Myodaiji-cho, Okazaki 444–8585, Japan.
M. Takeichi, Department of Biophysics, Faculty of Science, Kyoto University, Kitashirakawa, Kyoto 606–8502, Japan.

*To whom correspondence should be addressed. E-mail: nose@bio.phys.s.u-tokyo.ac.jp
‡Present address: Department of Physics, School of Science, University of Tokyo, 7-3-1 Hongo, Bunkyo-ku, Tokyo 113–8654, Japan.